Cancer Management and Research

Dovepress

open access to scientific and medical research

Open Access Full Text Article

ORIGINAL RESEARCH

# RETRACTED ARTICLE: miR-4429 Regulates the Proliferation, Migration, Invasion, and Epithelial-Mesenchymal Transition of Cervical Cancer by Targeting FOXM1

This article was published in the following Dove Press journal:
*Cancer Management and Research*

Lin Liang[1–3]
Yu Wei Zheng[1–3]
Yan Li Wang[1–3]

[1]Department of Pathology, Fudan University Shanghai Cancer Center, Shanghai 200032, People's Republic of China; [2]Department of Oncology, Shanghai Medical College, Fudan University, Shanghai 200032, People's Republic of China; [3]Institute of Pathology, Fudan University, Shanghai 200032, People's Republic of China





**Background:** miR-4429 acts as an inhibitor in many malignant tumors and participates in the biological processes of them, but the clinical value and potential molecular mechanism of miR-4429 in cervical cancer (CC) are still under investigation.

**Objective:** To analyze the clinical value and molecular mechanism of miR-4429 in CC.

**Materials and Methods:** A qRT-PCR assay was employed to determine the levels of miR-4429 and forkhead-box M1 (FOXM1) in CC tissues, CC cell lines (SiHa, CaSki, ME-180, and C33A) and human normal immortalized epithelial cell lines (HaCaT). The proliferation, migration, invasion, and apoptosis abilities of ME-180 and C33A cells were detected, and the epithelial-to-mesenchymal transition (EMT)-related proteins in the cells were also determined.

**Results:** MiR-4429 acted as a tumor suppressor gene in CC tissues and cells and was linked to lymph node metastasis, International Federation of Gynecology and Obstetrics (FIGO) staging. The survival analysis revealed that lymph node metastasis, high FIGO staging, and low miR-4429 expression were all related to the unfavorable prognosis of the patients, and the dual-luciferase reporter assay revealed that FOXM1 was the target of miR-4429. Both overexpression of miR-4429 and knock-down of FOXM1 inhibited the proliferation, migration, invasion, and EMT of CCCs, and accelerated the apoptosis of them. Conversely, both knockdown of miR-4429 and overexpression of FOXM1 promoted those biological behaviors of the cells. Moreover, the rescue experiment revealed that the overexpression of FOXM1 reversed the influences of miR-4429 overexpression on the proliferation, migration, invasion, and EMT of CCCs.

**Conclusion:** miR-4429 acts as a tumor suppressor in CC and can directly target FOXM1 to regulate the proliferation, migration, invasion, apoptosis and EMT of CCCs, so miR-4429 is expected to be a new therapeutic target for CC.

**Keywords:** miR-4429, FOXM1, cervical cancer, cell, biological behavior

Correspondence: Yu Wei Zheng
Department of Pathology, Fudan University Shanghai Cancer Center, Shanghai 200032, People's Republic of China
Tel +86- 21-64175590
Email zhengfeng413@163.com

Yan Li Wang
Department of Oncology, Shanghai Medical College, Fudan University, Shanghai 200032, People's Republic of China
Tel +86- 21-64175590
Email drwyl@126.com

## Introduction

Cervical cancer is one of the most prevalent female malignant tumors, with incidence and mortality both ranking second only to those of breast cancer in female malignant tumors worldwide. As the second female malignant tumor, it is also the malignant tumor with the highest incidence and mortality in developing countries.[1] It is estimated that there are about 500,000 new CC patients each year, of which about 280,000 patients die of CC.[2] CC is difficult to find in the early stage, which usually delays effective treatment.[3] Although radical operation, chemotherapy and radiotherapy are

submit your manuscript | www.dovepress.com
DovePress
http://doi.org/10.2147/CMAR.S244167

able to significantly prolong the survival time of patients, the prognosis of advanced CC patients is still unfavorable and the 5-year overall survival (OS) of them is only 40%.[4] Therefore, it is crucial to understand the molecular mechanism of CC and develop effective treatment strategies.

MicroRNA (miRNA) is a highly conserved small non-coding RNA that is able to specifically regulate gene expression.[5] MiRNA is related to the progress and metastasis of various human cancers and can act as an oncogene or a tumor suppressor gene in them.[6] Earlier previous studies have confirmed that as a key factor in many tumors, miRNA participates in various crucial cellular processes, including proliferation, migration, metastasis, and epithelial-mesenchymal transition (EMT).[7,8] Although the study of miRNA provides a new insight into the mechanism of CC,[9] there are still many aspects of it requiring further exploration. One previous study has pointed out that miR-4429 is a recognized anti-cancer miRNA,[10] which plays a negative regulatory role in the proliferation, growth, and differentiation of tumor cells, and interacts with proto-oncogene to main the relative stability of positive and negative regulatory signals.[11]

In glioblastoma cells, inhibiting miR-4429 expression can accelerate the growth of cancer cells and miR-4429 can be sponged by lymphocytic leukemia deletion gene to regulate Transcription factor SP1.[12] In CCCs, miR-4429 was down-regulated and can target DNA double strand break repair protein to make CC sensitive to radiation.[13] These studies enlighten us about potential molecular mechanosis and treatment with miR-4429 for tumor. In order to understand the clinical value and specific mechanism of miR-4429 in CC, we used TargetScan and miRDB databases, to search for the potential targets of miR-429. One of the interesting predicted targets was forkhead-box M1(FOXM1). According to some previous studies, FOXM1 plays a role in the development and progression of various tumors.[14] For example, highly expressed in liver cancer, FOXM1 can induce metastasis and growth of cancer cells and participates in the EMT of them.[15,16] Although both miR-4429 and FOXM1 play crucial roles in many cancers, their mechanism of action in CC still needs further research.

In this study, we analyzed the clinical value and molecular mechanism of miR-4429 in CC, with the goal of providing potential targets for clinical treatment of it.

## Materials and Methods

A total of 102 CC patients admitted to Shanghai Medical College, Fudan University from January 2013 to August 2014 were enrolled, and CC tissues and corresponding normal tumor-adjacent tissues were sampled from each of them. Inclusion criteria of the patients: Patients diagnosed with CC according to tissue biopsy, patients with clinical staging conforming to the CC staging standard of the International Federation of Gynecology and Obstetrics (FIGO), patients who had not received any cancer treatment before surgery, and patients with complete clinical data. The specimens were frozen and stored in liquid nitrogen at −80°C immediately after being collected for later analysis, and we carried out the study after obtaining informed consent forms from each patient and permission from the Ethics Committee of Shanghai Medical College, Fudan University. Exclusion criteria of the patients: Patients with expected survival time less than 3 months, patients with other cognoid malignant tumors, patients with autoimmune disease or hematologic disease, patients unable to cooperate with the study for mental disorder, patients who dropped out of the study, and those lost to follow up.

### Follow-Up

The patients were followed up by telephone, WeChat, and other means, once every 3 months.

Overall survival (OS) refers to the time from treatment to death or the last follow-up.

### Cell Culture

CC cell lines (CaSki, ME-180, C33A, and SiHa) and normal immortalized epithelial cell lines (HaCaT) from Shenzhen OTWO Biotechnology Co., Ltd. (China) were identified through short-sequence tandem repeat region analysis to confirm that they were free of mycoplasma contamination. After confirmation, the cells were cultured in dulbecco's modified eagle medium (DMEM) (Nobleryder Technology Co., Ltd., Beijing, China) containing penicillin-streptomycin (100 μg/mL) and 10% fetal bovine serum (FBS) in a 5%$CO_2$ incubator at 37°C.

### Cell Transfection

MiR-4429-mimics, miR-4429-inhibitor, negative control sequence miR-NC, PcDNA3.1 expression vector (sh-FOXM1), small interfering RNA (si-FOXM1), and corresponding negative control (sh-NC) were all synthesized by Shanghai Genechem Co., Ltd. (China). ME-180 and C33A cells were seeded into 6-well plates at $1\times10^5$ cells/well, and cultured until their confluency reached 70%-80%, and then the cells were transfected using a Lipofectamine 2000 kit (Invitrogen, Carlsbad,

California, the United States) according to kit instructions, with a final concentration of 50nM miRNA mimetic and siRNA. After 48 h of transfection, the cells were harvested, and the transfection efficiency was determined using a qRT-PCR. The assay was repeated three times.

## RNA Isolation and qRT-PCR

Total RNA was extracted from tissues and SiHa, CaSki, ME-180, C33A, and HaCaT cells with Trizol reagent (Shanghai Even Bridge Biotechnology Co., Ltd., China). The tissue mass used for RNA isolation was about 10 mg, and the number of cells was about $1 \times 10^6$. RNA sample (2 μL) was collected, and the RNA mass was detected using a spectrophotometer. The RNA concentration and optical density (OD) 260/OD280 were recorded. Its OD260/OD280 was 1.9–2.1, indicating a good purity. The integrity of extracted total RNA was detected by agarose gel electrophoresis. The sampled RNA was reversely transcribed into cDNA by a RevertAid First Strand cDNA Synthesis Kit (Shanghai Biotechnology Co., Ltd. China) under the instructions of the manufacturer. The RT reaction system consisted of 20 μL total volume containing 1 μL Total RNA, 4 μL 5 ×Reaction Buffer, 1 μL RNA enzyme inhibitor (20 U/μL), 2 μL 10 mM dNTP Mix, 1 μL M-MuLV reverse transcriptase, 1 μL miRNA RT, and RNase-free ddH2O added to adjust the volume. On the ABI7300 real-time PCR system (Thermo Fisher Scientific, Shanghai, China), the expression of genes was determined using SYBR Premix Ex Taq reagent (Invitrogen, Carlsbad, California, the United States) with U6 or GAPDH as internal control. qPCR amplification conditions: Pre-denaturation at 94°C for 3 mins, followed by 35 cycles of denaturation at 94°C for 30 s, annealing at 58°C for 30 s, and extension at 72°C for 45 s. The amplification efficiency was in the range of 95–105%, and the assay was repeated three times. The obtained data were studied using the $2^{-\Delta\Delta}$ method. The primers were all synthesized by Shanghai GenePharma Co., Ltd. (China), and the primer sequences were as follows: For miR-4429: Forward 5′-GGCCAGGCAGTCTGAGTTG-3′ and backward 5′-GGGAGAAAAGCTGGGCTGAG-3′; for FOXM1: Forward 5′-AGCGACAGGTTAAGGTTGAG-3′ and backward 5′-GTGCTGTTGATGGCGAATTG-3′; For U6: Forward 5′-CAAAGTCAGTGCAGGTAGGCTTA-3′ and backward 5′-AACGCTTCACGAATTTGCGT-3′, and for GAPDH: Forward 5′-CCTCGTCTCATAGACAAGATGGT-3′ and backward 5′-GGGTAGAGTCATACTGGAACATG-3′.

## Luciferase Reporter Gene Assay

Potential targets of miR-4429 were predicted based on TargetScan and miRDB databases.[18] WT-FOXM1 and Mut-FOXM1 plasmids were constructed. ME-180 and C33A cells were seeded into a 24-well plate at $5\times10^3$ per well, and transfected when their confluency reached 90%. OPTI-MEM medium (50 μL) was used to dilute 2 μL Lipofectamine 2000, mixed well, let to stand for 5 mins, and then mixed with diluted plasmid DNA. Subsequently, 100 ng recombinant vector, 50 ng plasmid, 50 nM miR-4429 mimics and miR-NC were diluted with 50 μL OPTI-MEM medium, and let to stand for 5 min, and the diluted plasmid DNA was mixed with diluted Lipofectamine 2000, and then let to stand for 20 min. Afterwards, the mixture (100 μL) was added to each well, and the DMEM was replaced after 6 hrs. After 48 hrs, the cells were collected, and washed with PBS once. Passive lysis solution (200 μL) was added into each well, and centrifuged at 12000g for 10 min. Supernatant (20 μL) was collected, and mixed with 100 μl luciferase assay reagent (Promega, Madison, Wi, USA). Subsequently, the firefly luciferase activity was detected with a fluorometer and its first reading was recorded. Then, 100 μ l Stop & Glo reagent was added into the supernatant, and mixed well within 10 min. Afterwards, the second reading was used as the luciferase activity of sea pansy. The assay was repeated three times, and the ratio of luciferase activity of firefly to luciferase activity of sea pansy was calculated.

## Cell Proliferation Assay

A cell counting kit-8 (CCK8) (Shanghai Beyotime Biotechnology Co., Ltd. (China)) was applied to detect the cell proliferation ability of ME-180 and C33A cells. The cells were transferred to a 96-well plate at $5\times10^3$ cells/well, and CCK-8 solution (10 μL) was added into each detection well at 24, 48, 72, and 96 hrs after culturing. After each addition of the solution, the plate was continuously incubated for 2 hrs. Subsequently, the OD of each well at 450 nm was measured by a Multiskan FC enzyme mark instrument (Thermo Fisher Scientific, Shanghai, China). The assay was repeated three times.

## Cell Migration and Invasion Assay

The migration and invasion abilities of ME-180 and C33A cells were determined using the Transwell chamber method as follows: 20 μ l Matrigel (stock solution was 9 mg/mL, and it was diluted with serum-free DMEM

solution at a ratio of 1:9) was diluted, and then the diluted matrigel was spread on the 8 μm-aperture transwell insert of the Transwell chamber, and the chamber was placed on a 24-well plate, and incubated at 37°C for 1 hr. Afterwards, the cells were transferred to the upper compartment at $1\times10^5$/well, and 500 μL DMEM (Wuhan Chundu Biotechnology Co., Ltd., China) with 20% FBS was added into the lower compartment, and then chamber was incubated in an incubator. After 24 hrs, the transwell insert was taken out, and the cells on the upper layer of microporous membrane were wiped off with cotton swabs, and the membrane was stained with crystal violet for 15 min after being immobilized with methanol for 30 min. The number of cells penetrating the microporous membrane in 5 randomly selected fields under an EVOS XL Core phase-contrast microscope (Thermo Fisher Scientific, Shanghai, China) was counted. The cell migration was evaluated according to the experiment steps in the invasion assay, except the coating step of Matrigel. The assay was repeated three times.

## Apoptosis Assay

The apoptosis ability of ME-180 and C33A cells was determined using the AnnexinV-FITC/PI as follow. Cells were digested with 0.1% trypsin after being trans fected for 48 hrs, and collected, and washed with PBS. About $1\times10^6$ cells were taken and seeded i o a 9 well plate. The Annexin V-FITC apoptosis a y kit (Wuhan Chundu Biotechnology Co., Ltd., China) was used to detect apoptosis according to its instructions. The labeled solution and FITC-labeled Annexin V were mixed at a ratio of 10:1, and the cells were resuspended with the mixed solution and incubated at room temperature in the dark for 30 min. After reaction with 5μL PI (50ug/mL) in the dark for 5 min, the suspension was added with 400 μL labeling solution, followed by cell apoptosis determination using an Attune NxT flow cytometer (Thermo Fisher Scientific Co., Ltd., Shanghai, China). A group of samples without Annexin V-FITC and PI were set as negative control group. The assay was repeated three times.

## Western Blot Assay

About $1\times10^7$ ME-180 and C33A cells were collected and lysed with Radio Immunoprecipitation Assay (RIPA) lysis buffer, and the total protein was extracted from them. The protein was quantified by a bicinchoninic acid (BCA) kit and its concentration was adjusted to 3μ g/μ l. The protein was separated using 10% sodium dodecyl sulfate-polyacrylamide gel electrophoresis (SDS-PAGE). The voltage was adjusted to 80V. When the sample entered the edge of the concentrated gel and separation gel (after electrophoresis for about 30 min), the voltage was adjusted to 120V. When the dye was about 1.0 cm away from the bottom of the rubber plate, electrophoresis was stopped (electrophoresis was carried out for about 90 min), and the gel was removed for subsequent analysis. The articles were transferred and placed in the order of filter paper, gel, and polyvinylidene fluoride (PVDF) membrane, with the filter paper from negative electrode to positive electrode. Electrotransformation was carried out in an ice bath, with voltage adjusted to 100 for 50 mins. The membrane was washed with TBST buffer solution three times, 5 mins each time, and then incubated with FOXM1 (1:500), E-Cadherin (1: 500), N-cadherin (1: 500), Vimentin (1: 500) and β-actin antibody (1:1000) at 4°C overnight. Afterwards, the membrane was washed with TBST buffer solution three times, 5 mins each time, cultured with horseradish peroxidase (HRP)-labeled goat anti-rabbit immunoglobulin G (IgG) secondary antibody at indoor temperature for 1 hr. After being washed with TBST buffer solution three times, 5 mins each time, the membrane was developed with electrochemiluminescence (ECL) solution. The brightness of target band was analyzed using the iBright Western blot imaging system (Thermo Fisher Scientific, Shanghai, China). Both kit and protein antibodies were purchased from Shanghai Beyotime Biotechnology Co., Ltd. (China). The assay was repeated three times.

## Statistical Analysis

In this study, the data were statistically analyzed using SPSS 17.0 and GraphPad Prism 6.0 (IBM, Armonk, New York, the United States). The miR-4429 expression in CC tissues and corresponding normal adjacent tissues were analyzed using the Mann–Whitney *U*-test. Enumeration data were expressed as percentage (%), and the correlation between miR-4429 and clinicopathological parameters was expressed by $\chi^2$. Survival curves of miR-4429 expression and CC patients were drawn through the Kaplan-Meier method, and the curve differences were analyzed through the log-rank method. Data about the expression at different time points were studied using the repeated measures analysis of variance, and post hoc pairwise comparison was carried out using the Bonferroni method. Moreover, Pearson's correlation analysis was conducted to analyze the correlation of

miR-4429 with FOXM1, and the univariate and multivariate Cox regression to analyze the factors affecting the prognosis of patients. P<0.05 implies a significant difference.

## Results

### miR-4429 Is Down-Regulated in CC Tissues and Related with Prognosis

A qRT-PCR was carried out to determine the 102 CC tissue specimens and 102 corresponding normal tumor-adjacent tissue specimens, and it came out that the miR-4429 expression decreased significantly in CC tissues (Figure 1A). In addition, high and low expression of miR-4429 were defined according to median miR-4429 expression to analyze the relationship between miR-4429 expression and clinicopathological features, and it was turned out that low miR-4429 expression was strongly linked to lymph node metastasis and high FIGO stage (Figure 1B and C and Table 1), and the low expression indicated a poor 5-year OS for CC patients (Figure 1D). Multivariate Cox regression revealed that high FIGO stage, lymph node metastasis, and low miR-4429 expression were prognostic factors for OS of the patients (Table 2).

### miR-4429 Affects Biological Behaviors of CCCs

For the purpose of exploring the role of miR-4429 in CC, we determined the miR-4429 expression in CC cell lines (CaSki, ME-180, C33A, and SiHa) and human normal immortalized epithelial cell line (HaCaT). It was turned out that compared with normal cell lines (HaCaT), SiHa, CaSki, ME-180 and C33A cell lines showed a significant



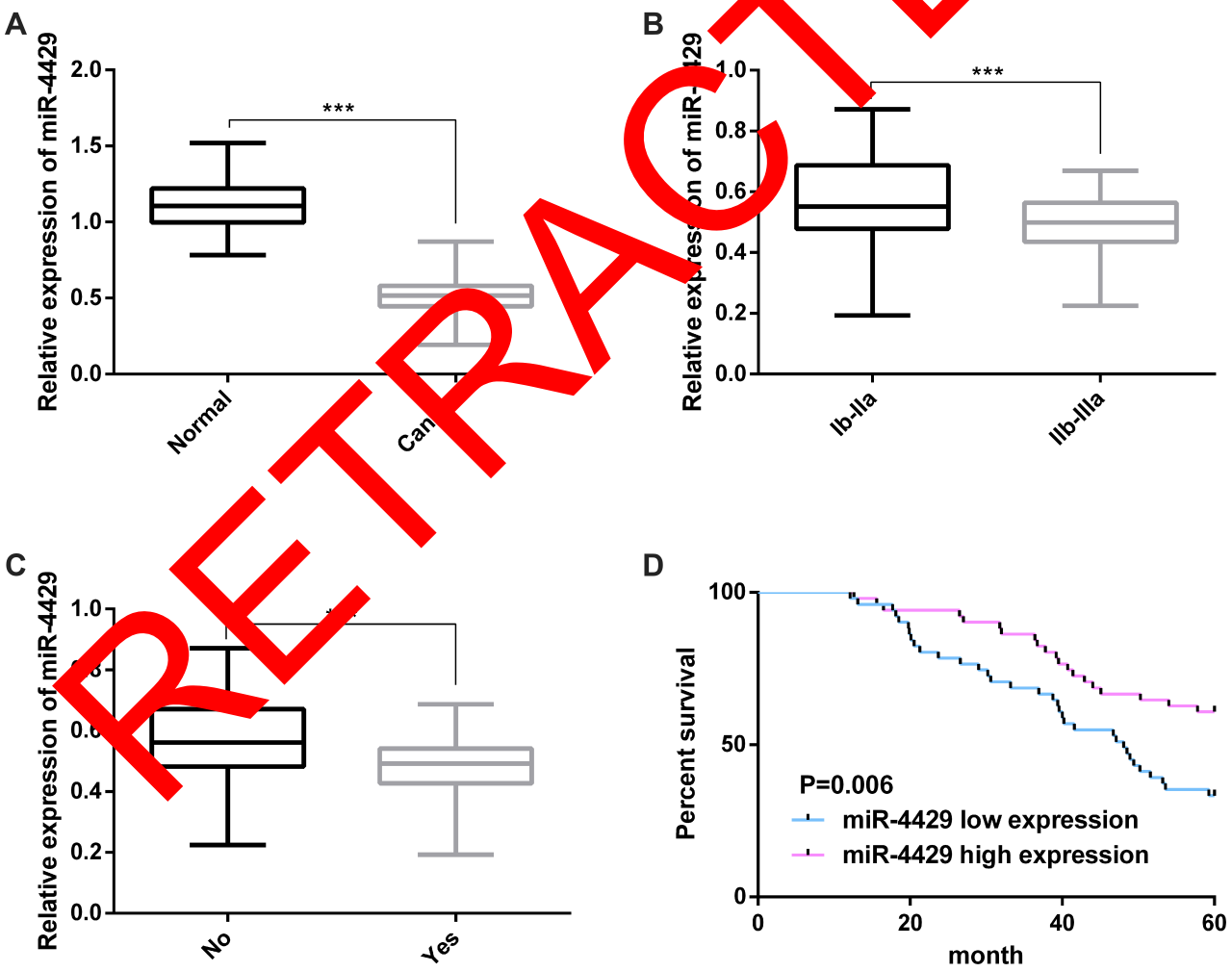


**Figure 1** miR-4429 was down-regulated in CC tissues and correlated with prognosis. (**A**) miR-4429 was greatly down-regulated in CC tissues; (**B**) The expression of miR-4429 in patients with different FIGO stages; (**C**) The expression of miR-4429 in patients with or without lymph node metastasis; (**D**) Survival curves of high and low miR-4429 expression.
**Note:** ***P<0.001.
**Abbreviation:** miR, microRNA.

**Table 1** Correlation of miR-4429 with Clinicopathological Features of CC Patients

| Clinicopathological Parameters | n | miR-4429 | | $\chi^2$ | P-value |
|---|---|---|---|---|---|
| | | Low Expression | High Expression | | |
| Age (Y) | | | | 0.362 | 0.548 |
| <50 | 43 | 20 (39.22) | 23 (45.10) | | |
| ≥50 | 59 | 31 (60.78) | 28 (54.90) | | |
| Histological type | | | | 2.590 | 0.108 |
| Adenocarcinoma | 42 | 25 (49.02) | 17 (33.33) | | |
| Squamous cell carcinoma | 60 | 26 (50.98) | 34 (66.67) | | |
| FIGO staging | | | | 7.016 | 0.008 |
| Ib-IIa | 39 | 13 (25.49) | 26 (50.98) | | |
| IIb-IIIa | 63 | 38 (74.51) | 25 (49.02) | | |
| Lymph node metastasis | | | | 68 | 0.001 |
| No | 47 | 17 (33.33) | 30 (58.82) | | |
| Yes | 55 | 34 (66.67) | 21 (41.18) | | |
| Pathological grading | | | | 14 | 0.088 |
| High/Moderate differentiation | 70 | 31 (60.78) | 39 (47) | | |
| Low differentiation | 32 | 20 (39.22) | 2 (23. | | |
| Invasive depth | | | | 1.998 | 0.158 |
| <1/2 | 41 | 17 (33.33) | 24 (47.06) | | |
| ≥1/2 | 61 | 34 (66.67) | 27 (5 94) | | |
| Tumor diameter (cm) | | | | 0.640 | 0.424 |
| <4cm | 44 | 20 (39 | (47.06) | | |
| ≥4cm | 58 | 31 (60. | 27 (52.94) | | |
| HPV infection | | | | 3.304 | 0.069 |
| Negative | 26 | 9 7.65) | 17 (33.33) | | |
| Positive | 76 | 4 82.35) | 34 (66.67) | | |

**Abbreviations:** miR, microRNA; CC, cervical cance GO, n of Gynecology and Obstetrics; HPV, human papillomavirus.

**Table 2** Univariate and Multivariate Cox R ession Analyses of Factors Affecting OS of the Patients

| Factor | Univariate | | Multivariate | |
|---|---|---|---|---|
| | HR (95CI%) | P-value | HR (95CI%) | P-value |
| Age (Y) | 1.1 (0.652–1.909) | 0.690 | | |
| Histological typ | .20 (0.672–1.968) | 0.609 | | |
| FIGO stagi | 1.999 (1.169–3.418) | 0.011 | 1.825 (1.056–3.156) | 0.031 |
| Lymph node m st | 2.304 (1.326–4.004) | 0.003 | 2.091 (1.188–3.680) | 0.011 |
| Pathological gradi | 1.493 (0.812–2.745) | 0.197 | | |
| Invasive depth | 1.347 (0.789–2.300) | 0.275 | | |
| Tumor diameter (cm) | 1.564 (0.914–2.677) | 0.103 | | |
| HPV infection | 1.082 (0.588–1.990) | 0.800 | | |
| MiR-4429 | 2.520 (1.437–4.417) | 0.001 | 2.048 (1.147–3.655) | 0.015 |

**Abbreviations:** HR, hazard ratio; CI, confidence interval; FIGO, Federation of Gynecology and Obstetrics; HPV, human papillomavirus; miR, microRNA.



down-regulation in miR-4429 expression (Figure 2A). We selected ME-180 and C33A cells whose miR-4429 expression was the lowest among that of the four cell lines for follow-up experiment, and applied qRT-PCR to evaluate the transfection efficiency, finding that compared with cells transfected with miR-NC, those transfected with miR-4429-

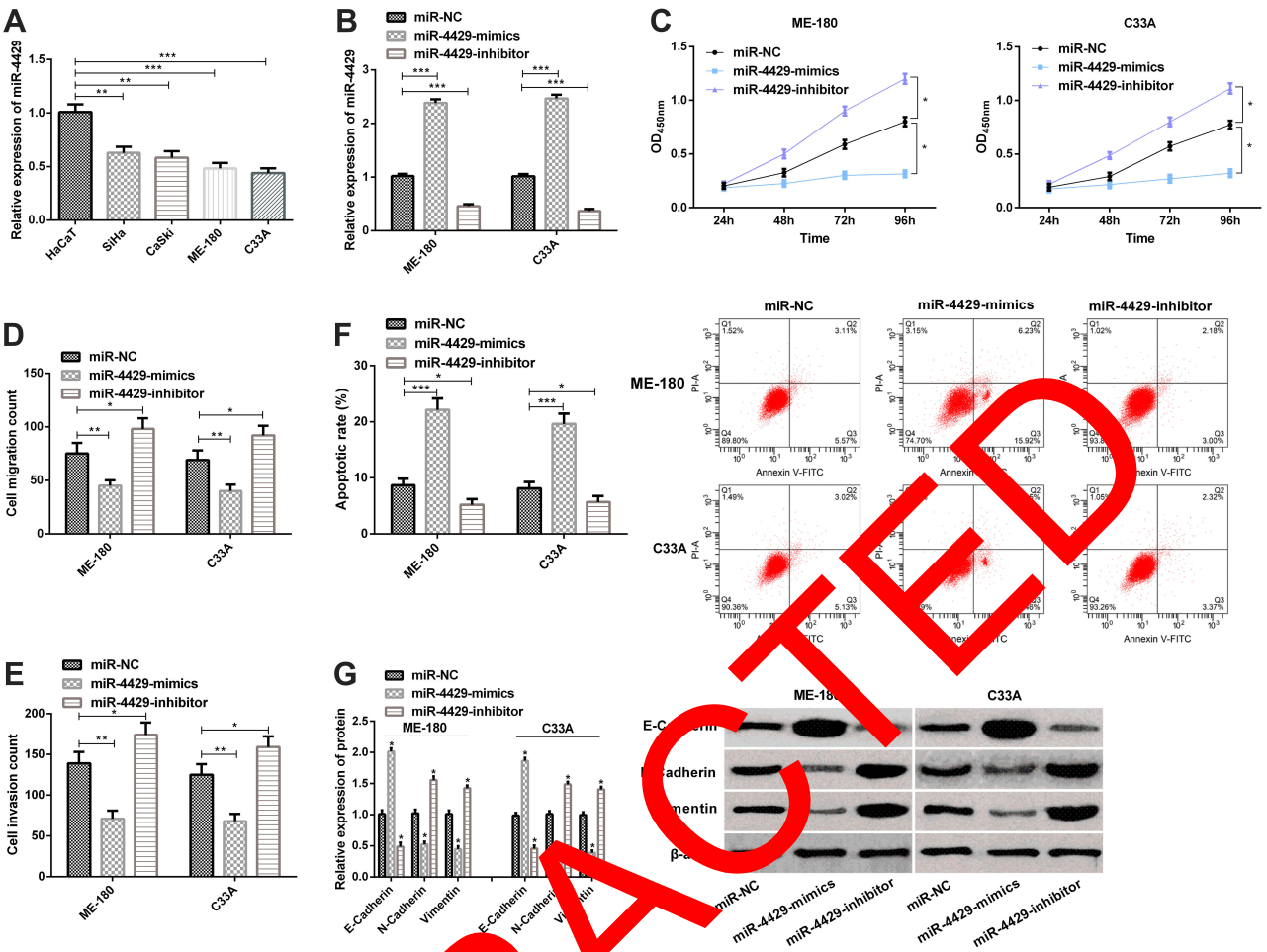




**Figure 2** miR-4429 affects biological behaviors of CCC (**A**) The ex ression of m 4429 in CC cell lines (SiHa, CaSki, ME-180, and C33A) and human normal immortalized epithelial cell line (HaCaT); (**B**) The expression of miR- 9 in cel with miR-NC, miR-4429-mimics, or miR-4429-inhibitor in qRT-PCR; (**C**) Proliferation of ME-180 and C33A cells in the CCK-8 assay; (**D**) Mi ion of and C33A in the migration assay; (**E**) Invasion of ME-180 and C33A in the invasion assay; F. Apoptosis of ME-180 and C33A in flow cytometry and ap osis map; (**G**) he expression of E-Cadherin, N-Cadherin, and Vimentin in the Western blot assay and protein bands.
**Notes:** *P<0.05; **P<0.01, and ***P<0.00
**Abbreviations:** miR, microRNA; OD ptical sity.

mimics showed si ficantl up-regulated miR-4429, while those transfected wi R-4429- ibitor showed significantly dow reg ated i R-44 (Figure 2B). Afterwards, we inv igated t influenc s of miR-4429 on the biological beha rs ME-18 and C33A. CCK-8 revealed that overexpressi of miR-4429 lowered the cell proliferation ability, while k ock-down of it enhanced the ability (Figure 2C), and the cell migration and invasion assay revealed that miR-4429 overexpression slowed down cell migration and invasion, while knockout of it resulted in opposite results (Figure 2D and E). What's more, the flow cytometry showed that overexpression of miR-4429-induced apoptosis, while knockout of it suppressed apoptosis (Figure 2F). We further analyzed the effects of miR-4429 on EMT-related markers. The Western blot assay revealed that overexpression of miR-4429 up-regulated the level of E-Cadherin, and significantly down-regulated the levels of N-Cadherin and Vimentin, and knockout of it gave rise to opposite results (Figure 2G).

## FOXM1 Interacts Directly with miR-4429

We selected potential target genes of miR-4429 based on TargetScan and miRanda databases, and found the following results. The bioinformatics analysis revealed that there were binding loci between miR-4429 and FOXM1, and the luciferase reporter gene analysis revealed that ME-180 and C33A cells co-transfected with WT-FOXM1 and miR-4429-mimics showed significantly lowered luciferase activity, while those co-transfected with Mut-FOXM1 and miR-4429-mimics showed no change in luciferase

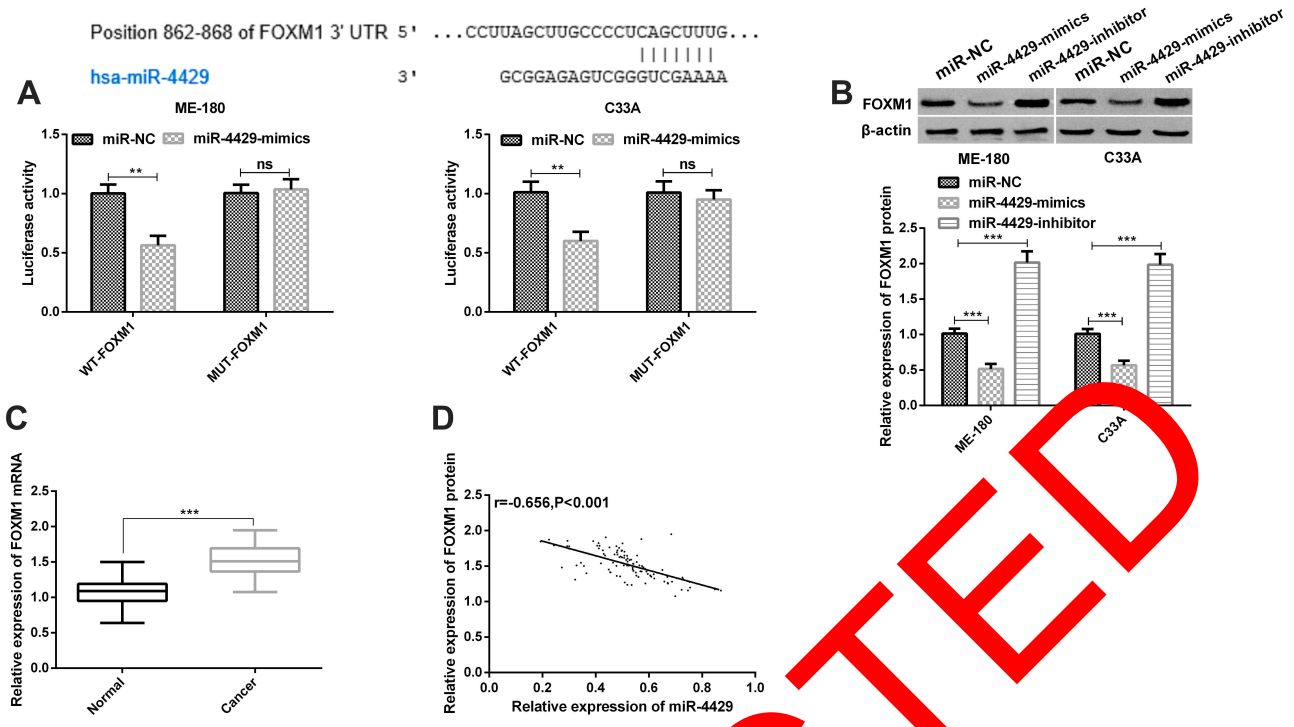


**Figure 3** FOXM1 was a target of miR-4429. (**A**) FOXM1 was a potential target gene of miR-44[illegible] according to the dual-luciferase reporter gene assay; (**B**) The expression of FOXM1 in ME-180 and C33A cells transfected with miR-NC, miR-4429-mimics, or miR-4429-[illegible]hibitor in the W[illegible]ern blot assay, and protein bands; (**C**) The expression of FOXM1 in clinical samples in the qRT-PCR assay; (**D**) miR-4429 was negatively correlated wi[illegible] FOXM1 in clinic[illegible]samples.
**Notes:** $^{ns}$P>0.05; **P<0.01 and ***P<0.001.
**Abbreviations:** FOXM1, Forkhead-box M1; miR, microRNA.



activity (Figure 3A). We evaluated the effects of miR-4429 on FOXM1 through a Western blot assay, finding that overexpression of miR-4429 gave rise to a significant decrease in FOXM1 expression in ME-180 and C33A cells, while knock-down of it gave rise to a significant increase in FOXM1 expression in the cells (Figure 3B). We also determined the level of FOXM1 in CC tissues and corresponding normal adjacent tissues through a qRT-PCR assay, finding that level of FOXM1 was high in CC tissues (Figure 3C). Pearson's correlation revealed that miR-4429 was negatively related to FOXM1 in CC tissues (Figure 3D).

## FOXM1 Affects Biological Behaviors of CCCs

For the purpose of understanding the role of FOXM1 in CC, we transfected sh-NC, si-FOXM1, and sh-FOXM1 into ME-180 and C33A cells, separately. The qRT-PCR assay for transfection efficiency revealed that compared with ME-180 and C33A cells transfected with sh-NC, those transfected with si-FOXM1 showed significantly decreased FOXM1 expression, while those transfected with sh-FOXM1 showed significantly increased FOXM1 expression (Figure 4A), and the CCK-8 assay, Transwell assay, and flow cytometry revealed that knock-down of FOXM1 weakened cell proliferation (Figure 4B), migration (Figure 4C), and invasion abilities (Figure 4D) of ME-180 and C33A cells, and promoted apoptosis of them (Figure 4E). On the contrary, overexpression of FOXM1 promoted cell proliferation, migration and invasion, and inhibit cell apoptosis. The Western blot analysis revealed that knock-down of FOXM1 gave rise to an increase in E-Cadherin level and a significant decrease in N-Cadherin and Vimentin levels, while overexpression of FOXM1 rise to a decrease in E-Cadherin level and a significant increase in N-Cadherin and Vimentin levels (Figure 4F).

### Up-Regulation of FOXM1 Can Reverse the Effects of miR-4429 Overexpression on the Biological Behaviors of CCCs

For the purpose of verifying that FOXM1 was regulated by miR-4429, we transfected miR-NC+sh-NC, miR-4429-mimics+sh-NC, and miR-4429-mimics+sh-FOXM1 into ME-180 and C33A cells, separately. The CCK-8 assay, Transwell assay, and flow cytometry revealed that

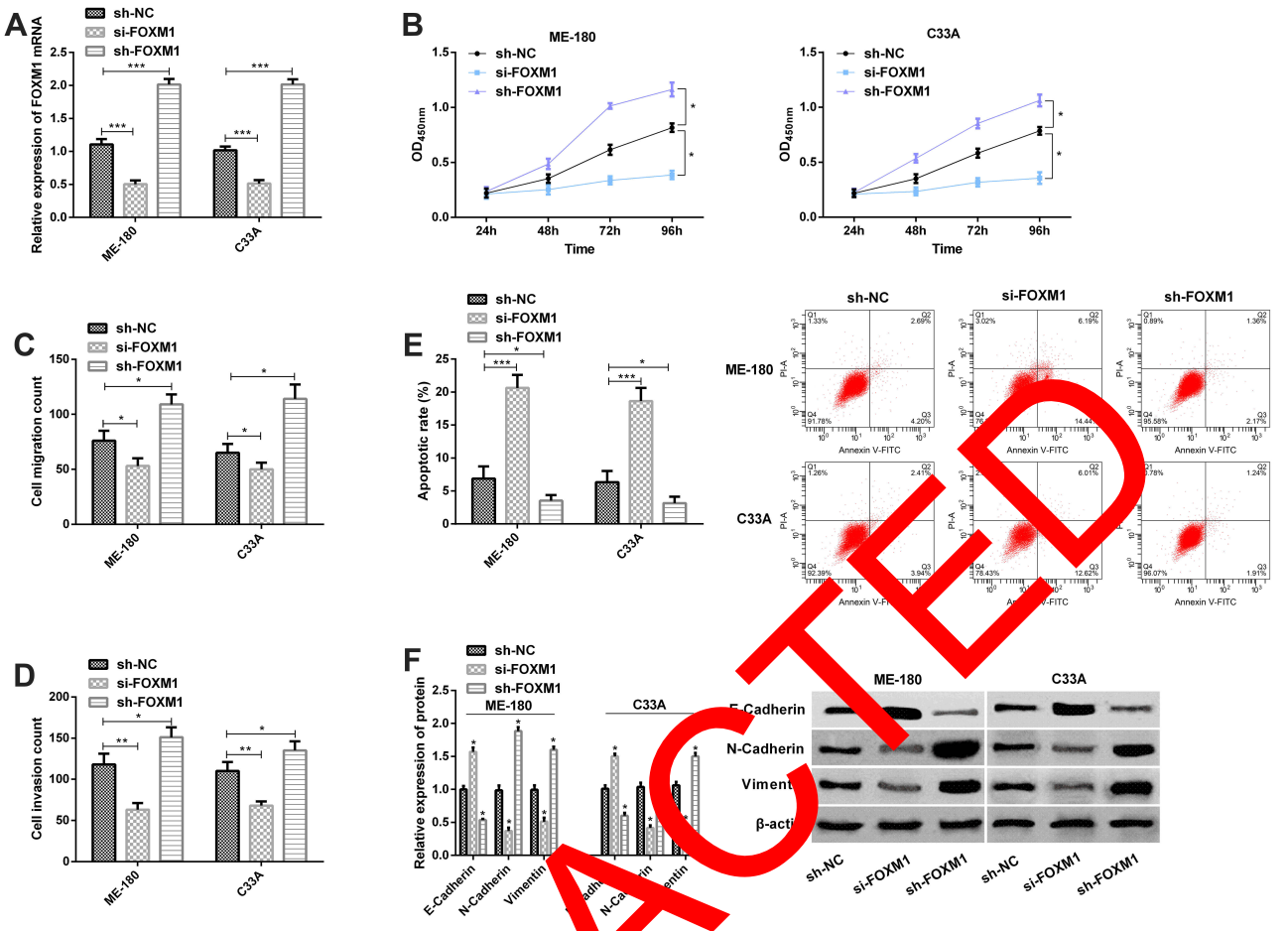


**Figure 4** FOXM1 affects biological behaviors of CCCs. (**A**) The expression of FOXM1 in ME-180 and C33A cells transfected with sh-NC, si-FOXM1 or sh-FOXM1 in the qRT-PCR assay; (**B**) Proliferation of ME-180 and C33A cells in the CCK-8 assay; (**C**) Migration of ME-180 and C33A cells in the migration assay; (**D**) Invasion of ME-180 and C33A cells in the invasion assay; (**E**) Apoptosis of ME-180 and C33A cells in the flow cytometry and apoptosis map; (**F**) The expression of E-Cadherin, N-Cadherin, and Vimentin in the Western blot assay and protein bands.

**Notes:** * P<0.05; **P<0.01, and ***P<0.001.

**Abbreviations:** FOXM1, Forkhead-box M1; OD, Optical density.



compared with ME-180 and C33A cells transfected with miR-4429-mimics or miR-NC, those transfected with sh-FOXM1+miR-4429-mimics showed accelerated proliferation (Figure 5A), migration (Figure 5B), and invasion (Figure 5C), and inhibited apoptosis (Figure 5D), and the Western blot assay revealed that the cells showed down-regulated E-Cadherin level and up-regulated N-Cadherin and Vimentin levels (Figure 5E). Compared with cells transfected with miR-NC+sh-NC, those transfected sh-FOXM1+miR-4429-mimics showed no significant changes in proliferation, migration, invasion, apoptosis and protein expression of E-Cadherin, N-Cadherin, and Vimentin. Those results implied that overexpression of FOXM1 played a major role in cell lines, which promoted cell proliferation, migration and invasion, and inhibits cell apoptosis. In addition, the experimental results of restoration of high-level FOXM1 masked the role of miR-4429-mimics in CCcs in functional analysis.

## Discussion

CC is a common malignant tumor in human beings.[19] In this study, miR-4429 was lowly expressed in CC tissues, and it was related to unfavorable prognosis of patients, and in in vitro experiments, overexpression of miR-4429 or knock down of its target gene FOXM1 could inhibit the proliferation, migration, invasion and EMT progression of CCCs and promote cell apoptosis. In addition, the experimental results of restoration of high-level FOXM1 masked the role of miR-4429-mimics in CCCs in functional analysis.

Previous studies have verified the importance of miR-4429 in tumor progression. For example, miR-4429 is

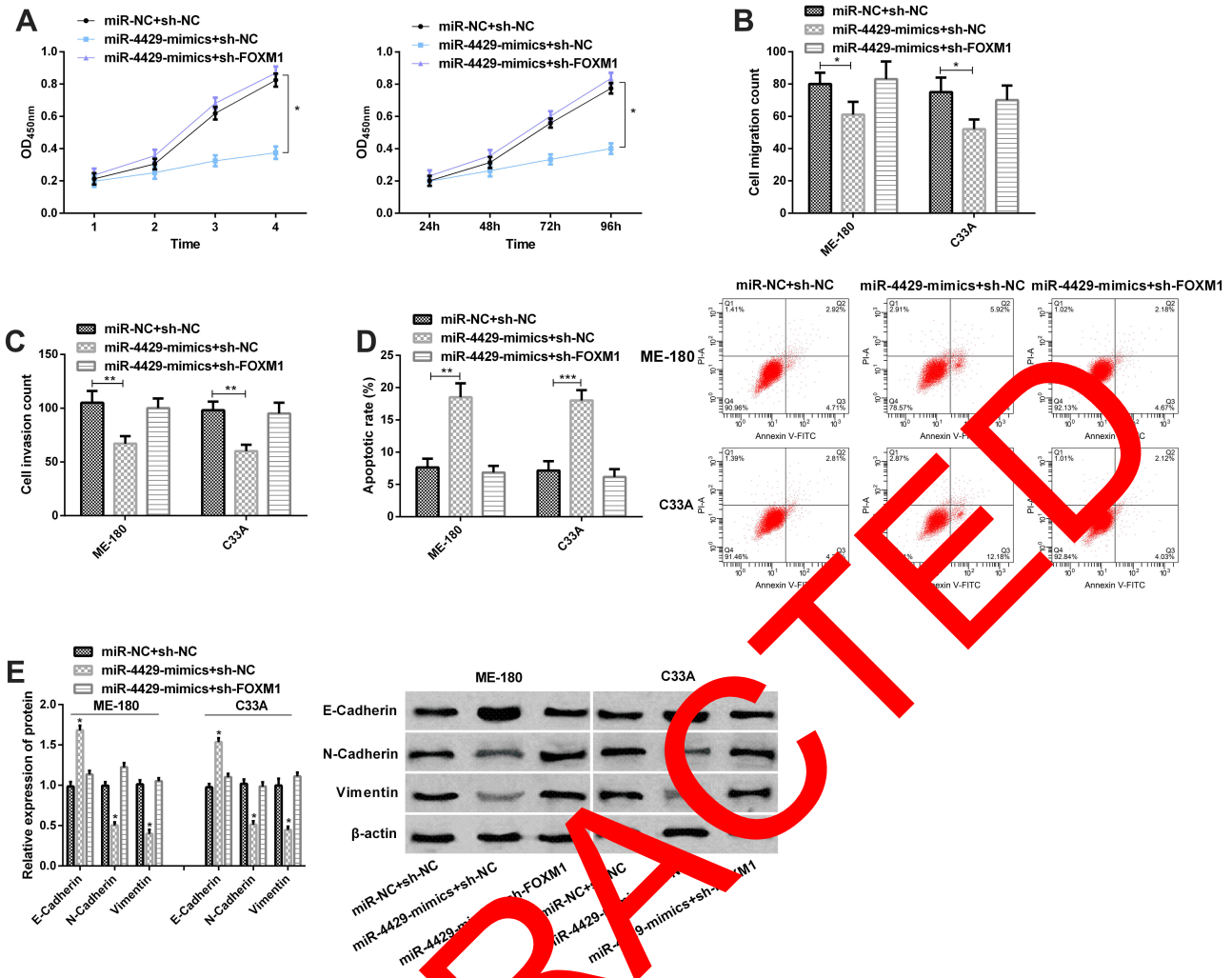




**Figure 5** Up-regulation of FOXM1 could reverse the effects of miR-4429 overexpression on the biological behaviors of CCCs. (**A**) Proliferation of ME-180 and C33A cells in the CCK-8 assay; (**B**) Migration of ME-180 and C33A cells in the migration assay; (**C**) Invasion of ME-180 and C33A cells in the invasion assay; (**D**) Apoptosis of ME-180 and C33A cells in the flow cytometry and apoptosis rate; (**E**) The expression of E-Cadherin, N-Cadherin, and Vimentin in the Western blot assay and protein bands.
**Notes:** *P<0.05; **P<0.01, and ***P<0.001.
**Abbreviations:** OD, Optical density; miR, microRNA; FOXM1, Forkhead-box M1.

underexpressed in gastric cancer, and able to slowdown its progression by targeting methyltransferase-like 3/transporters for protein precursors.[20] Our study showed that the expression of miR-4429 in CC tissues was significantly down-regulated compared with adjacent corresponding normal tissue specimens, which implied that miR-4429 could act as a tumor suppressor in CC. Our study also found that low expression of miR-4429 was related to lymph node metastasis, high FIGO staging, and poor prognosis of the patients, which implied that the deletion of miR-4429 expression may be linked to the occurrence and poor prognosis of CC. Therefore, miR-4429 is expected to be a new indicator for the prognosis evaluation of CC.

miRNA imbalance affects the progression of malignant tumors, such as differentiation, proliferation and angiogenesis.[21,22] We firstly verified the inhibitory function of miR-4429 in CC, and then analyzed the influences of miR-4429 on the biological behaviors of CCCs. It was turned out that like the miR-4429 expression in CC tissues, the expression of it was down-regulated in CCCs, and overexpression of it could inhibit proliferation, invasion, and migration of CCCs and induce apoptosis of them. Conversely, knockdown of miR-4429 could accelerate cell proliferation, migration, and invasion abilities, and inhibit cell apoptosis of the tumor. Similarly, one study by Pan et al[23] has reported that the miR-4429 expression decreases in clear cell renal cell carcinoma tissues and cells, and miR-4429 can slowdown the proliferation, migration, and invasion, and EMT of tumor cells after being up-regulated, and could suppress progression and

EMT of tumor cells through targeting cyclin-dependent kinase 6. One study has pointed out that EMT is essential in tumor metastasis, which is mainly characterized by the deletion of epithelial marker E-Cadherin, increase of interstitial markers Vimentin and N-Cadherin protein, and occurrence of migration and invasion behavior.[24] Our study revealed that overexpression of miR-4429 could hinder EMT, while knock-down of it could promote EMT and our study uncovered for the first time that miR-4429 could impact the migration, proliferation, invasion and EMT of CCCs. However, the exact mechanism of miR-4429 in the cancer still needs further research.

We analyzed the binding loci between miR-4429 and FOXM1 according to data from online database, and verified through double luciferase report that FOXM1 was a target of miR-4429. Earlier studies have verified the carcinogenic role of FOXM1 in tumors and the participation of it in EMT activation.[25–27] For example, one study by Li et al[28] has revealed that FOXM1 is overexpressed in non-small-cell lung carcinoma, and participated in EMT induced by transforming growth factor β1 (TGF-β1) and can be directly targeted by miR-134 to further inhibit EMT. It has also been reported that FOXM1 acts as a carcinogen in breast cancer and can be targeted by miR-671-5p to regulate the proliferation, invasion, cell cycle, and EMT of breast cancer cells.[29] In our study, knockdown of FOXM1 suppressed the migration, invasion, proliferation and EMT of CCCs, and accelerated apoptosis, and overexpression of FOXM1 gave rise to opposite results in those aspects. On the contrary, overexpression of FOXM1 promoted the proliferation, migration, invasion and EMT of CCCs and inhibited their apoptosis. The results suggest that FOXM1 plays an important role in CC. In CC, knock-down of FOXM1 can reverse the proliferation, migration, and invasion abilities of cancer cells caused by overexpression of miR-342-3p in CC.[30] Similarly, our rescue experiment also revealed that the up-regulation of FOXM1 could weaken the influences of miR-4429 overexpression on malignant phenotypes and EMT of CCCs. Therefore, miR-4429 is probably a new marker for CC treatment. Our study verified for the first time that miR-4429 could directly target FOXM1 to hinder the progression of CC. However, there are still some deficiencies in it. Firstly, there is only an in vitro experiment, but no in vivo experiment to verify the anti-tumor effect of miR-4429 in CC. Secondly, the clinical application of miR-4429 needs to be verified by clinical practice.

To sum up, miR-4429 acts as an inhibitor in CC and can directly target FOXM1 to affect the malignant phenotypes and EMT of CCCs. Therefore, miR-4429 is expected to become a new therapeutic target for CC.

## Disclosure

The authors report no conflicts of interest in this work.

## References


1. Arbyn M, Weiderpass E, Bruni L, et al. Estimates of incidence and mortality of cervical cancer in 2018: a worldwide analysis. *Lancet Glob Health*. 2019.
2. Peralta-Zaragoza O, Deas J, Meneses-Acosta A, et al. Relevance of miR-21 in regulation of tumor suppressor gene PTEN in human cervical cancer cells. *BMC Cancer*. 2016;16:215. doi:10.1186/s12885-016-2231-2
3. Zheng M, Hou L, Ma Y, et al. Exosomal let-7d-3p and miR-30d-5p as diagnostic biomarkers for non-invasive screening of cervical cancer and its precursors. *Mol Cancer*. 2019;18(1):76. doi:10.1186/s12943-019-09[illegible]-x
4. Zhang J, Yao T, Wang Y, Yu J, Liu Y, Lin Z. Long noncoding RNA MEG3 is downregulated in cervical cancer and affects cell proliferation and apoptosis by regulating miR-21. *Cancer Biol Ther*. 2016;17(1):104–113. doi:10.1080/15384047.2015.1108496
5. Nagy A, Lánczky A, Menyhart O, Gyorffy B. Validation of miRNA prognostic power in hepatocellular carcinoma using expression data of independent datasets. *Sci Rep*. 2018;8(1):9227. doi:10.1038/s41598-018-27521-y
6. Zhan MN, Yu XT, Tang J, et al. MicroRNA-494 inhibits breast cancer progression by directly targeting PAK1. *Cell Death Dis*. 2017;8(1):e2529. doi:10.1038/cddis.2016.440
7. Chhabra R. let-7i-5p, miR-181a-2-3p and EGF/PI3K/SOX2 axis coordinate to maintain cancer stem cell population in cervical cancer. *Sci Rep*. 2018;8(1):7840. doi:10.1038/s41598-018-26292-w
8. Tao P, Wen H, Yang B, Zhang A, Wu X, Li Q. miR-144 inhibits growth and metastasis of cervical cancer cells by targeting VEGFA and VEGFC. *Exp Ther Med*. 2018;15(1):562–568. doi:10.3892/etm.2017.5392
9. Chandrasekaran KS, Sathyanarayanan A, Karunagaran D. miR-214 activates TP53 but suppresses the expression of RELA, CTNNB1, and STAT3 in human cervical and colorectal cancer cells. *Cell Biochem Funct*. 2017;35(7):464–471. doi:10.1002/cbf.3304
10. Song W, Miao DL, Chen L. Comprehensive analysis of long non-coding RNA-associated competing endogenous RNA network in cholangiocarcinoma. *Biochem Biophys Res Commun*. 2018;506(4):1004–1012.
11. Lipsick J. A history of cancer research: tumor suppressor genes. *Cold Spring Harb Perspect Biol*. 2020;12(2):a035907. doi:10.1101/cshperspect.a035907
12. Liu X, Chen R, Liu L. SP1-DLEU1-miR-4429 feedback loop promotes cell proliferative and anti-apoptotic abilities in human glioblastoma. *Biosci Rep*. 2019;39(12). doi:10.1042/BSR20190994
13. Sun H, Fan G, Deng C, Wu L. miR-4429 sensitized cervical cancer cells to irradiation by targeting RAD51. *J Cell Physiol*. 2020;235(1):185–193. doi:10.1002/jcp.28957
14. Nandi D, Cheema PS, Jaiswal N, Nag A. FoxM1: repurposing an oncogene as a biomarker. *Semin Cancer Biol*. 2018;52(Pt 1):74–84. doi:10.1016/j.semcancer.2017.08.009
15. Chai N, Xie HH, Yin JP, et al. FOXM1 promotes proliferation in human hepatocellular carcinoma cells by transcriptional activation of CCNB1. *Biochem Biophys Res Commun*. 2018;500(4):924–929. doi:10.1016/j.bbrc.2018.04.201

16. Xiu G, Sui X, Wang Y, Zhang Z. FOXM1 regulates radiosensitivity of lung cancer cell partly by upregulating KIF20A. *Eur J Pharmacol*. 2018;833:79–85. doi:10.1016/j.ejphar.2018.04.021
17. Xu X, Zhu S, Tao Z, Ye S. High circulating miR-18a, miR-20a, and miR-92a expression correlates with poor prognosis in patients with non-small cell lung cancer. *Cancer Med*. 2018;7(1):21–31. doi:10.1002/cam4.1238
18. Zhang C, Zhang CD, Ma MH, Dai DQ. Three-microRNA signature identified by bioinformatics analysis predicts prognosis of gastric cancer patients. *World J Gastroenterol*. 2018;24(11):1206–1215. doi:10.3748/wjg.v24.i11.1206
19. Zhu Y, Han Y, Tian T, et al. MiR-21-5p, miR-34a, and human telomerase RNA component as surrogate markers for cervical cancer progression. *Pathol Res Pract*. 2018;214(3):374–379. doi:10.1016/j.prp.2018.01.001
20. He H, Wu W, Sun Z, Chai L. MiR-4429 prevented gastric cancer progression through targeting METTL3 to inhibit m(6)A-caused stabilization of SEC62. *Biochem Biophys Res Commun*. 2019;517(4):581–587. doi:10.1016/j.bbrc.2019.07.058
21. Li Y, Cui X, Li Y, Zhang T, Li S. Upregulated expression of miR-421 is associated with poor prognosis in non-small-cell lung cancer. *Cancer Manag Res*. 2018;10:2627–2633. doi:10.2147/CMAR.S167432
22. Wei W, Huo B, Shi X. miR-600 inhibits lung cancer via downregulating the expression of METTL3. *Cancer Manag Res*. 2019;11:1177–1187. doi:10.2147/CMAR.S181058
23. Pan H, Hong Y, Yu B, Li L, Zhang X. miR-4429 inhibits tumor progression and epithelial-mesenchymal transition via targeting CDK6 in clear cell renal cell carcinoma. *Cancer Biother Radiopharm*. 2019;34(5):334–341. doi:10.1089/cbr.2018.2697
24. Li Y, Zhang T, Qin S, et al. Effects of UPF1 expression on EMT process by targeting Ecadherin, Ncadherin, Vimentin and Twist in a hepatocellular carcinoma cell line. *Mol Med Rep*. 2019;19(3):2137–2143. doi:10.3892/mmr.2019.9838
25. Wan LY, Deng J, Xiang XJ, et al. miR-320 enhances the sensitivity of human colon cancer cells to chemoradiotherapy in vitro by targeting FOXM1. *Biochem Biophys Res Commun*. 2015;457(2):125–132. doi:10.1016/j.bbrc.2014.11.039
26. Bayraktar R, Ivan C, Bayraktar E, et al. Dual suppressive effect of miR-34a on the FOXM1/eEF2-kinase axis regulates triple-negative breast cancer growth and invasion. *Clin Cancer Res*. 2018;24(17):4225–4241. doi:10.1158/1078-0432.CCR-17-1959
27. Chen L, Wu M, Ji C, Yuan M, Liu C, Yin Q. Silencing transcription factor FOXM1 represses proliferation, migration, and invasion while inducing apoptosis of liver cancer stem [illegible] regulating the expression of ALDH2. *IUBMB Life*. 20[illegible]
28. Li J, Wang Y, Luo J, et al. miR-134 i[illegible]bits epithelial to [illegible]esenchymal transition by targeting FOXM1 in non-sm[illegible]cell lung canc[illegible] cells. *FEBS Lett*. 2012;586(20):3761–3765. [illegible]:10.1016/j[illegible]bslet.2012[illegible]9.016
29. Tan X, Fu Y, Chen L, [illegible] al. miR-671-5p [illegible]nhibits epithelial-to-mesenchymal transition b[illegible]ownregul[illegible]ng FOXM1 expression in breast cancer. *Oncotarget*. 2016;7([illegible]293[illegible]07. doi:10.18632/oncotarget.6344
30. Li XR, Chu HJ, [illegible]T, Wang [illegible]Kong SF[illegible]ai SZ. miR-342-3p suppresses prolife[illegible]n, migration a[illegible]inv[illegible]on by targeting FOXM1 in human ce[illegible]cal [illegible]cer. *FEBS [illegible]ett*. 2014;588(17):3298–3307. doi:10.1016/j.febslet.2[illegible]07.020